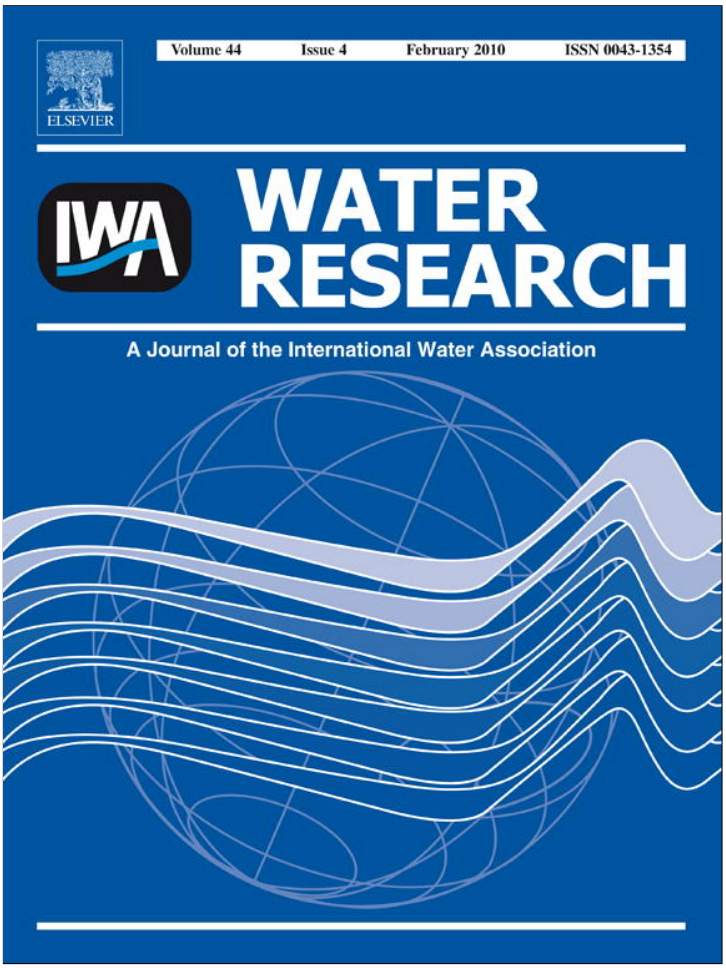

WATER RESEARCH 44 (2010) 1050–1061

Available at www.sciencedirect.com

journal homepage: www.elsevier.com/locate/watres

Modeling water flow and bacterial transport in undisturbed lysimeters under irrigations of dairy shed effluent and water using HYDRUS-1D

Shuang Jiang [a,*], *Liping Pang* [b], *Graeme D. Buchan* [a], *Jiří Šimůnek* [c], *Mike J. Noonan* [a], *Murray E. Close* [b]

[a] *Faculty of Agriculture and Life Sciences and CSEQ, PO Box 84, Lincoln University, Lincoln 7647, Canterbury, New Zealand*
[b] *Institute of Environmental Science & Research, PO Box 29-181, Christchurch, New Zealand*
[c] *Department of Environmental Sciences, University of California Riverside, CA, USA*

ARTICLE INFO

Article history:
Received 29 March 2009
Received in revised form
23 July 2009
Accepted 27 August 2009
Available online 2 September 2009

Keywords:
Modeling
Dual porosity
Bacterial transport
Undisturbed lysimeter
HYDRUS-1D

ABSTRACT

HYDRUS-1D was used to simulate water flow and leaching of fecal coliforms and bromide (Br) through six undisturbed soil lysimeters (70 cm depth by 50 cm diameter) under field conditions. Dairy shed effluent (DSE) spiked with Br was applied to the lysimeters, which contained fine sandy loam layers. This application was followed by fortnightly spray or flood water irrigation. Soil water contents were measured at four soil depths over 171 days, and leachate was collected from the bottom. The post-DSE period simulations yielded a generally decreased saturated water content compared to the pre-DSE period, and an increased saturated hydraulic conductivity and air-entry index, suggesting that changes in soil hydraulic properties (e.g. via changes in structure) can be induced by irrigation and seasonal effects. The single-porosity flow model was successful in simulating water flow under natural climatic conditions and spray irrigation. However, for lysimeters under flood irrigation, when the effect of preferential flow paths becomes more significant, the good agreement between predicted and observed water contents could only be achieved by using a dual-porosity flow model. Results derived from a mobile-immobile transport model suggest that compared to Br, bacteria were transported through a narrower pore-network with less mass exchange between mobile and immobile water zones. Our study suggests that soils with higher topsoil clay content and soils under flood irrigation are at a high risk of bacteria leaching through preferential flow paths. Irrigation management strategies must minimize the effect of preferential flow to reduce bacterial leaching from land applications of effluent.

1. Introduction

Applying dairy shed effluent (DSE) onto land to fertilize pasture and dispose of effluent is a permitted activity in New Zealand. However, the use of inappropriate irrigation practices could result in an increased risk of contaminating waterways and groundwater with DSE. For example, high fecal coliforms were detected in the groundwater underlying soils treated with DSE and pasturing dairy cows plus flood irrigation at an area in South Canterbury (Close et al., 2008).

* *Corresponding author*. Tel.: +64 21 2179922; fax: +64 3 3423689.
E-mail address: shuang.jiang@msn.com (S. Jiang).
0043-1354/$ – see front matter © 2009 Elsevier Ltd. All rights reserved.
doi:10.1016/j.watres.2009.08.039

Table 1 – Soil properties of the lysimeters.

Lysimeter	Depth (cm)	Clay (%)	Silt (%)	Sand (%)	Bulk density ($g\,cm^{-3}$)	Porosity	Texture class[a]	Organic matter (%)	pH
A	0–20	20	50	30	1.09	0.58	Silt loam	6.72	4.41
	20–35	17	50	33	1.19	0.55	Silt loam		
	35–50	10	58	32	1.42	0.46	Silt loam		
	50–70	6	47	48	1.46	0.45	Sandy loam		
B	0–20	7	56	37	1.27	0.51	Silt loam	6.21	4.97
	20–35	8	52	40	1.23	0.53	Silt loam		
	35–50	6	40	54	1.44	0.46	Sandy loam		
	50–70	3	33	64	1.45	0.45	Sandy loam		
C	0–20	20	55	25	1.22	0.53	Silt loam	7.24	5.75
	20–35	9	56	35	1.28	0.52	Silt loam		
	35–50	9	56	35	1.43	0.46	Silt loam		
	50–70	5	33	62	1.54	0.42	Sandy loam		
D	0–20	9	57	33	1.19	0.54	Silt loam	7.18	4.72
	20–35	14	66	20	1.20	0.55	Silt loam		
	35–50	10	55	35	1.59	0.40	Silt loam		
	50–70	10	49	41	1.53	0.42	Loam		
E	0–20	10	57	33	1.17	0.55	Silt loam	6.30	4.66
	20–35	9	56	35	1.16	0.56	Silt loam		
	35–50	6	42	52	1.40	0.47	Sandy loam		
	50–70	6	48	46	1.32	0.50	Sandy loam		
F	0–20	9	55	36	1.03	0.60	Silt loam	6.07	4.11
	20–35	8	54	38	1.25	0.53	Silt loam		
	35–50	10	55	36	1.54	0.42	Silt loam		
	50–70	7	46	47	1.48	0.44	Sandy loam		

a McLaren and Cameron (1996). The organic matter and pH are for the top 10 cm only.

Knowledge of the fate and transport of bacteria in structured soils is crucial for assessing the risks for groundwater quality of land-applied animal effluent and wastes. Contaminant transport models can be very useful tools for the quantitative assessment of microbial transport in soils and to elucidate the important factors and processes that control microbial transport. With some assumptions, complex processes are reduced to a set of mathematical equations with parameters characterizing the system.

Although bacterial transport in intact soils has been investigated (Smith et al., 1985; Hekman et al., 1995; McMurry et al., 1998; Aislabie et al., 2001; McLeod et al., 2001, 2003, 2004; Guber et al., 2005), most of these studies do not include modeling work. Most reported studies on modeling bacterial transport are with repacked homogenous porous media (Hijnen et al., 2005; Bradford et al., 2006; Gargiulo et al., 2008; Torkzaban et al., 2008). Comparatively fewer studies (Shelton et al., 2003; McGechan and Vinten, 2003; Pang et al., 2008) have carried out modeling of bacterial transport through undisturbed soils. However, data used for modeling in these studies were largely obtained from experiments carried out indoors under simulated rainfall (Shelton et al., 2003; Pang et al., 2008). This may not be fully representative of behavior under natural climatic conditions and irrigation.

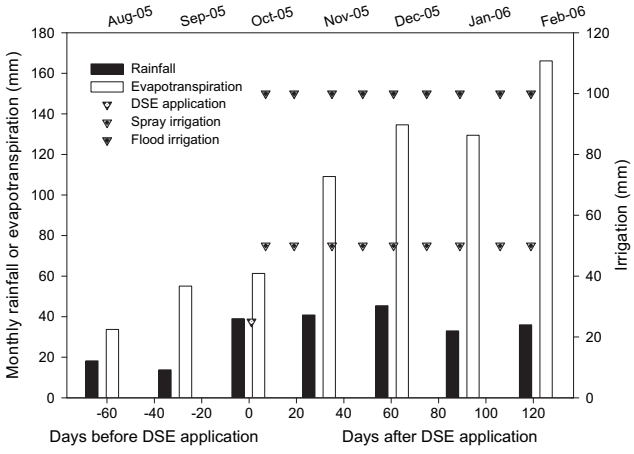

Fig. 1 – Comparison of rainfall, evapotranspiration (ET) and irrigation between pre- and post-DSE application periods.

Classically, water flow through variably-saturated soils is described by the Richards' equation with a uniform flow domain (Šimůnek and van Genuchten, 2008). Recently, efforts have been made at simulating contaminant transport under the influence of preferential flow using dual-porosity models (Gerke and van Genuchten, 1993, 1996; Šimůnek et al., 2001, 2003; Jarvis, 2007; van Genuchten and Šimůnek, 2004; Šimůnek and van Genuchten, 2008). These dual-porosity models assume the coexistence of two separate pore domains: fractures (or interaggregate pores, cracks and macropores); and matrix pores, with water exchange between the two domains. A few types of dual-porosity model have been incorporated into HYDRUS-1D (Šimůnek et al., 1998, 2005), the most extensively used model for simulating water and contaminant transport in variably-saturated porous media.

Our objective in this paper is, using HYDRUS-1D as a tool, to develop our understanding of (a) the dynamic changes of soil

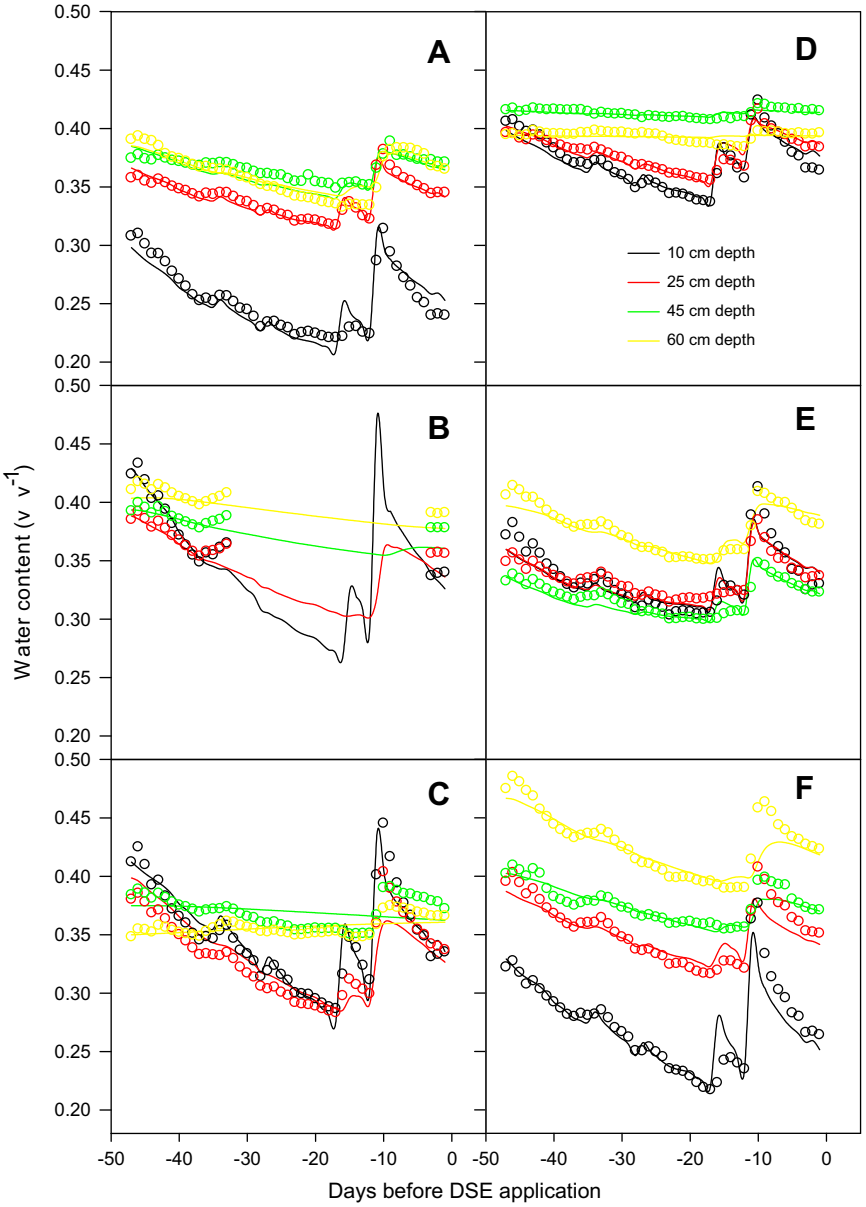

Fig. 2 – Comparison of water contents observed during the pre-DSE application period and predicted using the single-porosity flow model. Predicted values are in solid lines and observed values in empty circles. Black-depth 10 cm, red-depth 25 cm, green-depth 45 cm, and yellow-depth 60 cm. Same for Figs. 3–5. Note that a large portion of data was missing for lysimeter B due to instrument failure.

structure (as reflected in parameters of soil hydraulic properties) under different irrigation regimes and climatic conditions, and (b) the effect of preferential flow on water flow and bacterial transport. Based on our findings, recommendations were also provided for management strategies to minimize the risk of bacterial leaching through soils into groundwater.

2. Materials and methods

2.1. *Leaching experiments and experimental data*

The six lysimeters (50 cm diameter by 70 cm depth) used in this study were originally collected in 1996 from a dairy farm near Lincoln. The soil is an alluvial Templeton fine sandy loam with lithologic units of silt loam and sandy loam, with texture mostly coarser towards the lysimeter base (Table 1). Soil properties determined from destructive sampling at the end of this study are also listed in Table 1. These lysimeters were previously used for a study of nitrogen leaching from DSE until 2002. The lysimeters were located outdoors in the ground alongside an open trench at Lincoln University's Centre for Soil and Environmental Quality site. The lysimeters had a typical New Zealand pasture mix of ryegrass and white clover. Pasture was cut periodically to simulate typical grazing practice.

Rainfall was recorded automatically at the site using a tipping bucket gauge connected to a datalogger (Campbell

Table 2 – Hydraulic parameters optimized from observed water contents using the single-porosity flow model.

Lysimeter	Pre-application							Post-application						
	θ_r (v v^{-1})	θ_s (v v^{-1})	α (m^{-1})	n	Ks (m d^{-1})	SSRs	R^2	θ_r (v v^{-1})	θ_s (v v^{-1})	α (m^{-1})	n	Ks (m d^{-1})	SSRs	R^2
A	0.147	0.361[a]	0.080	1.942	7.119	0.023	0.978	0.042	0.308	1.340	1.300	6.339	0.435	0.565
	0.056	0.440	0.210	1.176	7.000			0.103	0.348	0.800	1.305	7.128		
	0.007	0.457	0.274	1.123	0.252			0.000	0.349	0.286	1.415	1.993		
B	0.003	0.465[a]	0.783	2.831	0.014	0.124	0.938							
	0.088	0.466	2.672	1.352	0.199									
	0.158	0.439	4.203	1.241	0.507									
C	0.076	0.452[a]	2.479	1.697	0.121	0.165	0.836	0.058	0.382	0.634	1.788	1.168	0.377	0.626
	0.051	0.415	5.623	1.338	0.223			0.065	0.366	0.600	1.829	7.000		
	0.001	0.375	5.512	2.423	0.000			0.128	0.350	0.267	1.606	3.370		
D	0.010	0.424[a]	0.682	1.596	0.008	0.084	0.916	0.027	0.418	0.601	1.788	7.000	0.288	0.728
	0.004	0.415	0.118	1.641	2.672			0.173	0.430	0.343	1.959	0.268		
	0.085	0.395	0.189	1.909	1.414			0.202	0.404	0.617	1.654	0.313		
E	0.133	0.415[a]	0.114	1.243	0.160	0.075	0.929							
	0.150	0.377	0.112	1.221	0.565									
	0.000	0.402	0.011	2.120	0.000									
F	0.001	0.380[a]	0.771	3.125	0.006	0.037	0.965	0.049	0.358	1.428	2.638	1.405	0.202	0.803
	0.039	0.418	0.691	2.280	1.316			0.007	0.368	1.045	2.298	1.989		
	0.025	0.485	0.928	1.872	0.006			0.014	0.393	1.255	3.714	0.484		

SSRs and R^2 values are for the whole lysimeter. Calibration of the single-porosity flow model was failed for post-application of lysimeters B and E.
a is not optimized but use maximum observed value.

Scientific, USA). Potential evapotranspiration data were obtained from the Broadfield climate station, located about 2 km north of the lysimeter site. In this study each lysimeter had a single soil moisture (TDR) sensor and temperature sensor at each of four depths (10, 25, 45 and 60 cm). Sensor data were collected with a datalogger and monitoring under natural climatic conditions commenced on 14 August 2005. More detailed information is contained in Jiang et al. (2008).

On 30 September 2005, 25 mm of DSE (spiked with NaBr) collected on the same day was applied to all lysimeters in 5 min (Jiang et al., 2008). The chemical characteristics of the DSE were Br 312 mg L^{-1}, fecal coliform 1.65×10^4 cfu mL^{-1}, total N 220 mg L^{-1}, total C 1612 mg L^{-1}, electric conductivity 1.56 mS cm^{-1} and pH 8.5. Fecal coliforms were not detected in the leachate collected prior to the leaching experiments. The lysimeters were irrigated with water on the 6th day after DSE application and every two weeks afterwards. The experiments were carried out for a period of 124 days. Flood irrigation (100 mm applied in 0.5 h on a 14-day cycle, extreme case) was applied to lysimeters B and E, which had very similar soil properties (Table 1) with sandy loam appearing at much shallower depth (35 cm) than in other lysimeters (50 cm depth). Spray irrigation (50 mm applied in 1.5 h on a 14-day cycle, a typical practice used in the region) was applied to the other four lysimeters. Irrigation and climatic data are given in Fig. 1.

Leachate samples were collected intensively in the first 12 h after DSE application. After 12 h, samples were taken once a day if available. During heavy rain, leachate was sampled as it became available. Leachate was collected under sterilized conditions. The bacterial samples were analyzed within 12 h of sampling using the Membrane Filtration Technique (APHA, 1998) with mFC agar (Difco™). The Br samples were analyzed using a Bromide Ion-Selective Electrode (ISE, Orion 250A 96-35 BN, Thermo Scientific, Inc.).

2.2. HYDRUS-1D model simulations

2.2.1. Boundary conditions and root water uptake

For Hydrus-1D model input, measured potential evapotranspiration (PET) was converted to potential evaporation rate (PE) and potential transpiration rate (PT) based on the following equation (Ritchie, 1972):

$$PE = PET \times \exp(-rExtinct \times LAI) \quad (1)$$

$$PT = PET - PE \quad (2)$$

Here rExtinct is a canopy extinction coefficient. A rExtinct value of 0.6 is adopted from Ludlow (1985) for ryegrass, which was the predominant vegetation for our lysimeters. Similarly, Hay and Porter (2006) reported a rExtinct value of 0.59–0.60 for wheat. LAI is leaf area index, generally LAI = 3 for grassland, adopting from Hay and Porter (2006) and Ludlow (1985). However the LAI value was adjusted according to the health status of the grass. For example, we used LAI = 2 for lysimeter F because there was some vegetation loss due to grass grub. A time-variable upper boundary condition was applied at the plant-atmosphere interface, with irrigation incorporated into rainfall data.

The bottom of each lysimeter had an added 20–30 mm thick layer of gravel. The base was sealed except for a central drainage hole, open to the atmosphere, for collecting drainage samples. No suction was applied to the base when samples were taken. Water drained from the bottom only when it was saturated, thus mathematically it was a seepage face at the lower boundary

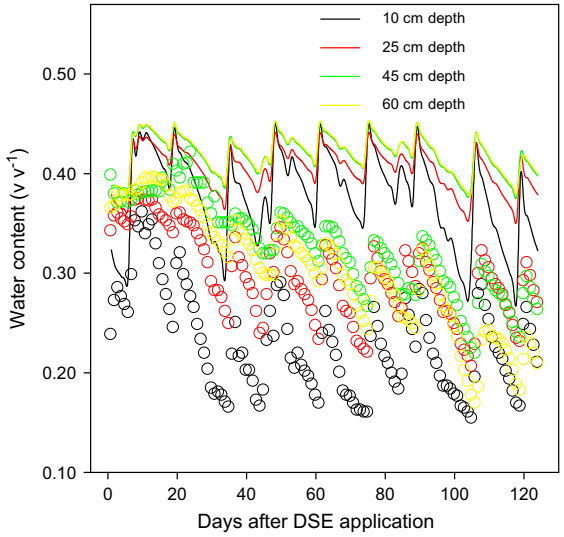

Fig. 3 – An example (lysimeter A) of the departure of predicted soil water contents from those observed for the post-DSE application period, due to direct application of parameter values derived from the pre-DSE application period. A single-porosity model was used for both periods.

(Flury et al., 1999). The saturated depth at the bottom, a few mm, was effectively the depth of the capillary fringe. The root zone depth observed, during destructive sampling at the end of the study, was about 40 cm, with most roots between 5 and 10 cm depths. During destructive sampling at the end of the study, we observed that more roots were distributed near the top and root density gradually reduced with depth. Therefore we assumed a linear distribution of root water uptake (from 1 to 0 from top to bottom of the root zone), with uptake decreasing linearly with depth. This allows more loss at the surface and no root uptake at the bottom of the root zone. The function of Feddes et al. (1978) was employed for root water uptake in HYDRUS-1D (Šimůnek et al., 1998, 2005).

2.2.2. *Water content simulations using the single-porosity flow model*

Measured soil moisture contents were simulated using the modified form of the Richards' equation (Šimůnek et al., 1998, 2005) for water movement in unsaturated soils under one-dimensional uniform flow:

$$\frac{\partial\theta}{\partial t} = \frac{\partial}{\partial z}\left[K(h)\left(\frac{\partial h}{\partial z} + 1\right)\right] - S \tag{3}$$

Here θ is volumetric water content [−], h is the soil water pressure head [L], t is time [T], z is the soil depth [L], and S is the sink term for root water uptake [T^{-1}]. The unsaturated hydraulic conductivity K [LT^{-1}], as a function of h, is given in the van Genuchten Equation (van Genuchten, 1980)

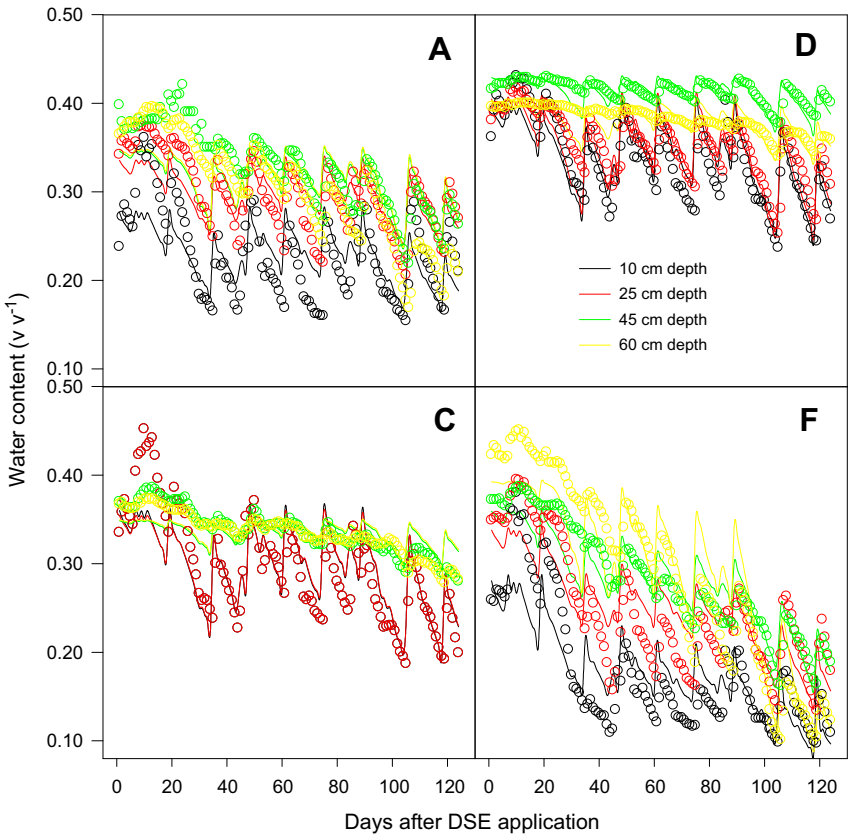

Fig. 4 – Comparison of soil water contents predicted from the calibrated single-porosity flow model and those observed during the post-DSE application period, for lysimeters A, C, D and F (spray irrigation).

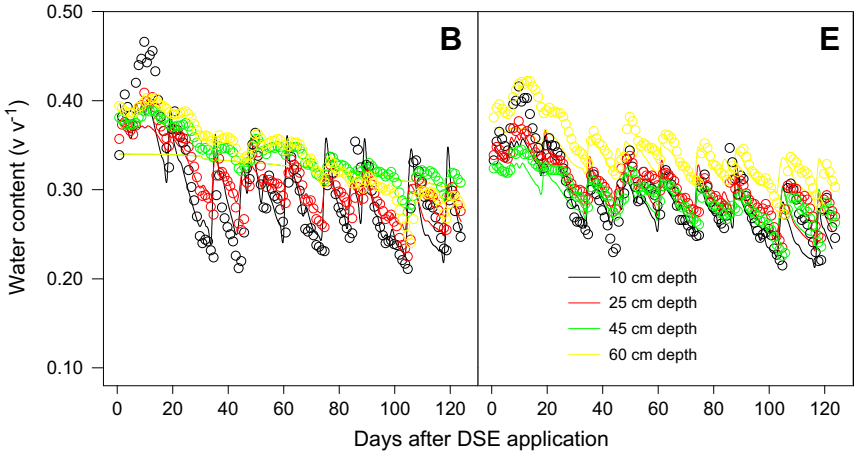

Fig. 5 – Comparison of observed soil water contents with those predicted from the dual-porosity flow model during the post-DSE application period, for lysimeters B and E (flood irrigation).

$$\theta(h) = \begin{cases} \theta_r + \dfrac{\theta_s - \theta_r}{\left[1 + |\alpha h|^n\right]^m} & h < 0 \\ \theta_s & h \geq 0 \end{cases} \quad (4)$$

$$K(h) = K_s S_e^l \left[1 - \left(1 - S_e^{1/m}\right)^m\right]^2 \quad (5)$$

and

$$m = 1 - 1/n \quad (n > 1) \quad (6)$$

θ_r and θ_s denote the residual and saturated volumetric water contents, respectively; K_s is the saturated hydraulic conductivity [LT^{-1}]; S_e is effective saturation; l is the pore connectivity parameter and is about 0.5 on average for many soils (Mualem, 1976); n is an empirical parameter related to the pore-size distribution, that is reflected in the slope of water retention curve; and α is an empirical parameter, often assumed to be related to the inverse of the air-entry suction (L^{-1}). Water retention curves of coarse-textured soils are generally sharp with steep slopes, thus high n values. A high α value (e.g. for sands and gravels) implies that soils de-saturate quickly at small suctions, while a low α value (e.g. for clays) indicates a slow de-saturation with increasing suctions.

Values of θ_r, θ_s, α, n and K_s were optimized by inverse modeling of water contents measured at four depths using the van Genuchten-Mualem single-porosity model from HYDRUS-1D. As HYDRUS allows a maximum of 15 parameters to be optimized, we reduced four soil layers (Table 1) to three layers by combining two soil layers that had similar textural compositions and water content patterns. The combined layer varied for different lysimeters. The initial inputs of θ_r, θ_s, α, n and K_s were estimated from measured water retention data (i.e. h vs. θ) using RETC (van Genuchten et al., 1991), or from the pedotransfer functions (PTFs) based on soil texture (% of sand, silt and clay) and bulk density using the Rosetta package (Schaap et al., 2001), which is embedded in HYDRUS-1D. Initial water contents measured were used as the inputs for initial water contents in the model. Values of θ_r, θ_s, α, n and K_s optimized from the pre-DSE application model were used as initial inputs for the post-DSE application model. To reduce the uncertainty of fitted parameters, we fixed saturated water contents using measured maximum water contents for the topsoil for the pre-DSE period simulations, reducing to a total of 14 parameters to be optimized.

2.2.3. *Water content simulations using the dual-porosity flow model*

For lysimeters B and E, the above single-porosity flow model failed to simulate the water contents measured during the

Table 3 – Hydraulic parameters optimized from water contents observed during the post-DSE application period using the dual-porosity flow model for lysimeters B and E (flood irrigaiton).

Lysimeter	Layer	θ_s (v v^{-1})	Ks (m d^{-1})	α (m^{-1})	n	ω (d^{-1} m^{-1})	SSRs	R^2
B	L_1	0.255	2.659	0.367	1.168	0.014	0.403	0.627
	L_2	0.160	2.963	0.085	1.173	0.003		
	L_3	0.039	2.028	0.002	1.526	0.000		
E	L_1	0.069	1.768	0.988	1.591	0.008	0.293	0.730
	L_2	0.093	1.428	1.007	1.294	0.003		
	L_3	0.048	5.462	0.367	1.797	0.001		

SSRs and R^2 values are for the whole lysimeter.

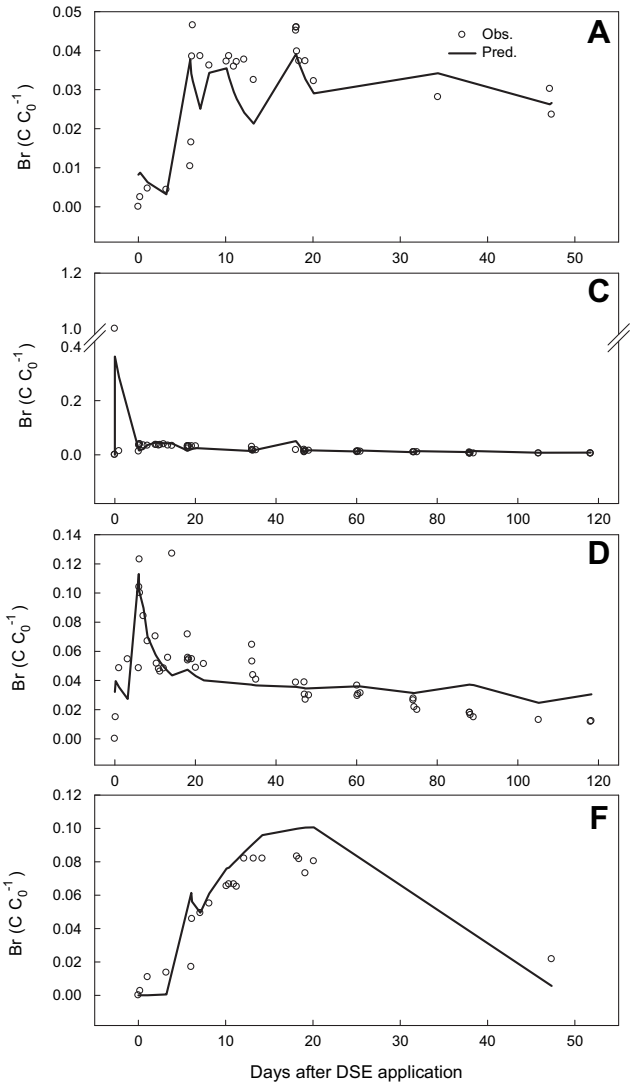

Fig. 6 – Br concentrations observed and predicted from the MIM transport model and the single-porosity flow model, in drainage from lysimeters A, C, D and F (spray irrigation).

post-DSE application period. During destructive sampling at the end of the field study, we observed that these two lysimeters contained much larger macropores than the other lysimeters. To consider the significant effect of preferential flow on these two lysimeters, a dual-porosity flow model (based on mass transfer driven by differences in soil water pressure head) was selected from HYDRUS-1D.

The dual-porosity formulation for water flow is based on a mixed formulation of the Richards equation to describe water flow in the macropores (mobile water region) and a mass balance equation to describe moisture dynamics in the matrix (immobile water region), as follows (Šimůnek et al., 2003):

$$\frac{\partial \theta_m}{\partial t} = \frac{\partial}{\partial z}\left[K(h)\left(\frac{\partial h}{\partial z}+1\right)\right] - S_m - \Gamma_w \tag{7}$$

$$\frac{\partial \theta_{im}}{\partial t} = -S_{im} + \Gamma_w \tag{8}$$

Here subscripts m and im refer to the mobile and immobile water regions, respectively; $\theta = \theta_m + \theta_{im}$ is the volumetric moisture content [–], S_{im} and S_m are sink terms (root water uptake) for both regions [T^{-1}], and Γ_w is the transfer rate for water exchange between macropores and matrix [T^{-1}]. We assume that root water uptake is preferentially from macropores, thus $S_{im} = 0$.

In the dual porosity flow model based on mass transfer driven by differences in soil water pressure head, the exchange rate of water between the macropores and matrix regions, Γ_w, is assumed to be proportional to the difference in pressure heads between the two pore regions (Gerke and van Genuchten, 1993; Šimůnek et al., 2003):

$$\Gamma_w = \omega(h_m - h_{im}) \tag{9}$$

Here ω is a first-order mass transfer coefficient ($L^{-1}T^{-1}$). Since pressure heads are now needed for both regions, this approach requires estimating retention curves for both pore regions. That means each region has its own values of θ_r, θ_s, α, and n. As a result, soil hydraulic properties are now described by six parameters for macropores (θ_r, θ_s, α, n, K_s, l), four parameters for the matrix ($\theta_{r\text{-}im}$, $\theta_{s\text{-}im}$, α_{im}, n_{im}), and a parameter (ω) for mass transfer between the two zones (Šimůnek et al., 2003). Note that the soil total saturated water content (e.g. $\theta_s + \theta_{s-im}$) can be obtained from measurement. To reduce the number of parameters optimized (maximum 15), we assumed that there is no residual water in macropores and matrix (i.e. $\theta_r = 0$, $\theta_{r\text{-}im} = 0$) and that the matrix is made of less permeable media with known values of $\theta_{s\text{-}im}$, α_{im}, and n_{im}, which were determined from soil texture and bulk density using Rosetta package. Therefore five parameters (θ_s, K_s, α, n, and ω) were optimized for each soil layer (total 15 parameters). Sometimes, θ_s or K_s were set at their measured values, or as reference values, as a constraint to reduce the simulation uncertainty.

2.2.4. *Simulations of bacteria and Br transport using the mobile-immobile contaminant transport model (MIM)*

Regardless of whether a single- or dual-porosity model is chosen for the water flow, HYDRUS-1D allows simulation of contaminant transport using a two-region mobile–immobile model, MIM (van Genuchten & Wagenet, 1989), The MIM assumes that contaminant transport is limited to the mobile water region and that water in the immobile water region is stagnant, with a first-order diffusive exchange process between the two regions (Šimůnek et al., 2003, 2005).

As there was no instantaneous sorption of bacteria in our data and Br is non-reactive, the following simplified MIM (Šimůnek and van Genuchten, 2006, 2008) was used in this study for simulating bacteria and Br transport:

$$\frac{\partial \theta_m C_m}{\partial t} = \frac{\partial}{\partial z}\left(\theta_m D_m \frac{\partial C_m}{\partial z}\right) - \frac{\partial q C_m}{\partial z} - \phi_m - \Gamma_s \tag{10}$$

$$\theta_{im}\frac{\partial C_{im}}{\partial t} = -\phi_{im} + \Gamma_s \tag{11}$$

Here C is the concentration in the liquid phase [ML^{-3}]; D is the dispersion coefficient [L^2T^{-1}], which is the product of dispersivity ξ[L] and pore-water velocity V (LT^{-1}), i.e. $D = \xi v$; q is the water flux [LT^{-1}]; φ_m and φ_{im} are reaction terms in the

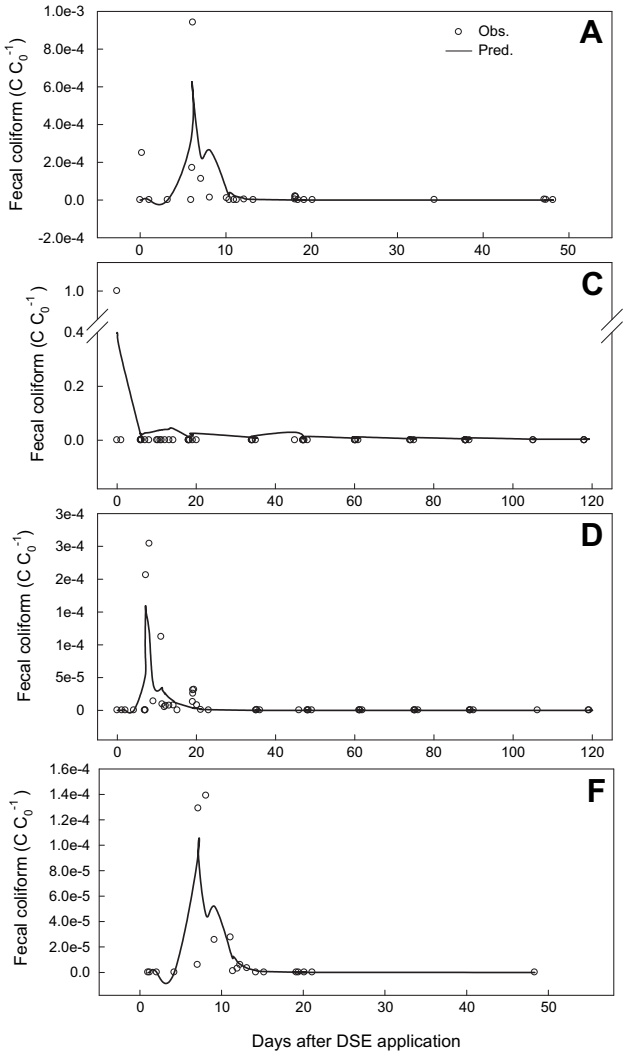

Fig. 7 – Fecal coliform concentrations observed and predicted from the MIM transport model and the single-porosity flow model, in drainage from lysimeters A, C, D and F (spray irrigation).

mobile and immobile domains [$ML^{-3}T^{-1}$], respectively ($\varphi_m = \varphi_{im} = 0$ for Br), and Γ_s is the term for mass transfer between the two regions [$ML^{-3}T^{-1}$].

The reaction terms (φ_m and φ_{im}), which represent any mechanisms responsible for removal of bacteria from the liquid phase (i.e. inactivation, or sorption to the solid phase or air-water interfaces), are defined as follows:

$$\phi_m = k_a\theta_m C_m + k_{aa}\theta_m C_m + \mu\theta_m C_m = (k_a + k_{aa} + \mu)\theta_m C_m = \lambda\theta_m C_m \quad (12)$$

$$\phi_{im} = k_a\theta_{im} C_{im} + k_{aa}\theta_{im} C_{im} + \mu\theta_{im} C_{im} = (k_a + k_{aa} + \mu)\theta_{im} C_{im} = \lambda\theta_{im} C_{im} \quad (13)$$

Here k_a is the attachment coefficient to the solid phase (T^{-1}), k_{aa} is the attachment coefficient to the air-water interfaces (T^{-1}), μ is the inactivation rate (T^{-1}), and $\lambda = k_a + k_{aa} + \mu$ is the lumped total removal rate (T^{-1}). Note that k_{aa} is equal to zero when a single-porosity flow model is used with MIM since in this case there is no air-phase present in the immobile zone.

When a single-porosity flow model is used with MIM, mass transfer between the two regions is through diffusion

$$\Gamma_s = \alpha_s(C_m - C_{im}) \quad (14)$$

where α_s is the first-order solute mass transfer coefficient (T^{-1}). When a dual-porosity flow model is used with MIM, contaminant is assumed to be able to move in and out of the matrix domain by diffusive and convective fluxes, and the term for mass transfer between the two regions, Γ_s, is written as (Šimůnek and van Genuchten, 2008):

$$\Gamma_s = \alpha_s(C_m - C_{im}) + \Gamma_w C* \quad (15)$$

where C^* is equal to C_m for $\Gamma_w > 0$ and C_{im} for $\Gamma_w < 0$.

The observed patterns of Br and bacterial transport were distinctively different (Figs. 6 and 7), due to size-exclusion in bacterial transport. Therefore transport parameters for bacteria were estimated independently from those for Br. Values of ξ, θ_{im} and α_s were optimized for Br data, while ξ, θ_{im}, λ and α_s were optimized for bacterial data. The values of hydraulic property parameters optimized from water flow were fixed during simulations of Br and bacteria. As their concentrations for model calibration were obtained from only one sampling location (i.e. the column base), we assumed that parameter values were the same for all soil layers. We also assumed when using the MIM model that while the immobile water content, θ_{im}, could differ for different soil layers, the porosity of the mobile domain was the same in all layers. HYDRUS-1D code was modified in this study to include these assumptions.

For lysimeters B and E, the dual-porosity flow model was used and properties of mobile and immobile water domains have been already defined from water content simulations. Thus we no longer needed to optimize θ_{im} for Br and bacterial transport. Therefore values of ξ and α_s were optimized for Br data, while ξ, λ and α_s were optimized for bacterial data.

3. Results and discussion

3.1. Water contents

3.1.1. Pre-DSE application period

Fig. 2 shows that soil water contents predicted from the single-porosity flow model fit well with those observed during the pre-DSE application period for all lysimeters. This is reflected in the very low values of SSRs (the Sum of Squared Residuals) (0.02–0.17) and very high values of R^2 (0.84–0.99) as shown in Table 2. Although 15 parameters were optimized simultaneously, there was little correlation between parameters, indicating they are relatively independent. The dual-porosity model was also applied for the pre-DSE application period but the results (not shown) were much worse. During this period, no irrigation was applied and lysimeters received only natural precipitation. Minor preferential flow is expected without irrigation (Chen et al., 2002). These results suggest that the effect of preferential flow was not significant for water movement during the pre-DSE application period and a single-porosity flow model is

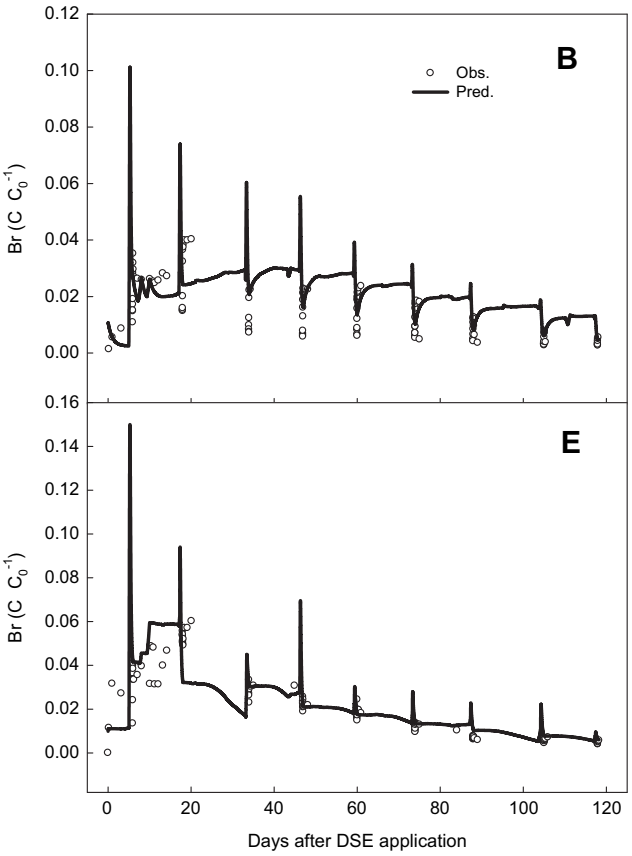

Fig. 8 – Br concentrations observed and predicted from the MIM transport model and the dual-porosity flow model, in drainage from lysimeters B and E (floor irrigation).

adequate for describing water movement in the absence of irrigation for the soils investigated.

3.1.2. *Post-DSE application period*

Using parameter values obtained from the pre-DSE application period for the post-DSE application period, the predicted water contents (without any calibrations) from the single-porosity model are all significantly higher than those observed. An example is given in Fig. 3 for lysimeter A. The discrepancies indicate that soil hydraulic properties had significantly changed and soils did not hold as much water as they did in the pre-DSE application period. If soil hydraulic properties had remained the same, irrigation should have resulted in a much wetter soil profile, which is opposite to what was observed.

Compared to the pre-DSE application period, the major changes in the post-DSE application period (refer to Fig. 1) were fortnightly irrigation events (100 mm for flood irrigation and 50 mm for spray irrigation) and drier and hotter climate conditions (spring and summer) than the pre-DSE application period (winter). Irrigation is more likely to generate preferential flow compared to rainfall (Chen et al., 2002). When applied in dry conditions (especially on the surface) and before the soil can wet up and swell, irrigation makes soil prone to have more preferential flow due to prior shrinkage and water repellence (Edwards et al., 1993; Jarvis, 2007; Lin and Zhou, 2008). Thus when irrigation water is applied, especially flood irrigation, much of the water could go through preferential flow, bypassing the matrix and draining deeper into the profile. Hotter and drier weather would promote the formation of macropores (Brown et al., 2000; Jarvis, 2007). This is especially true for soils with higher topsoil clay content (Jiang et al., 2008; Lin and Zhou, 2008) as clay may shrink and crack. All these facts would reduce the effective soil water holding capacity.

The single-porosity flow model was also successful for simulating water contents for the post-DSE application for lysimeters A, C, D, and F. Although it gave greater *SSRs* values (0.20–0.44) and lower R^2 values (0.57–0.80) than those from the pre-DSE application period ($SSRs = 0.02$–0.17, $R^2 = 0.84$–0.99), the post-DSE application period (124 days) was much longer than the pre-DSE application period (47 days). Statistically the goodness-of-fit for both data series has the same significance ($P = 0.000$).

The calibrated model for the post-DSE application period yielded generally decreased values of θ_s but increased values of α and K_s (Table 2) compared to those calibrated from the pre-DSE application period. This further supports the above evaluation on the change of soil hydraulic properties. As more macropores are developed, soil conductivity increases (higher K_s), more air-entry (greater α) is allowed, and less water is held (smaller θ_s).

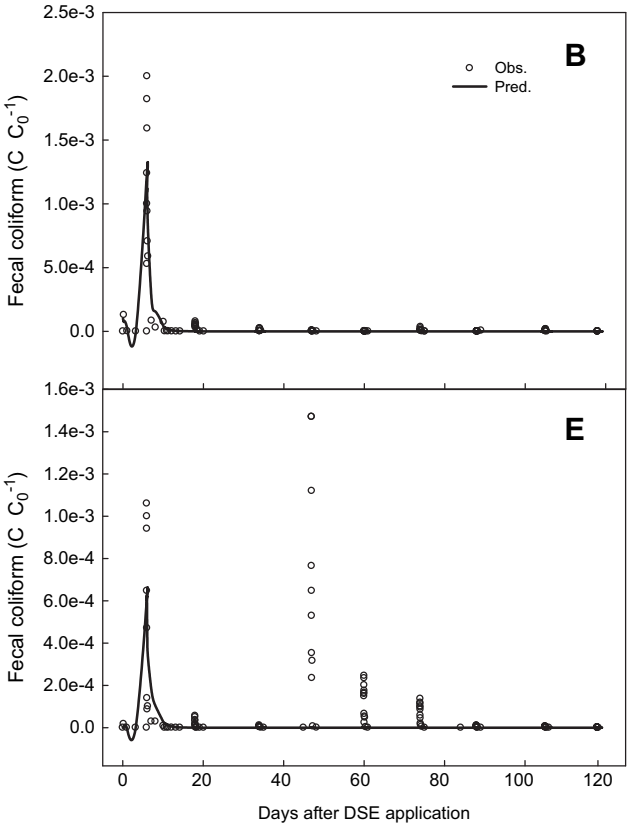

Fig. 9 – Fecal coliform concentrations observed and predicted from the MIM transport model and the dual-porosity flow model, in drainage from lysimeters B and E (floor irrigation).

Table 4 – Transport parameters optimized from observed Br and bacterial concentrations using the mobile-immobile transport model and single-porosity flow model for lysimeters A, C, D and F.

Lysimeter	Br					Fecal coliform					
	ξ(m)	θ_{im} (v v^{-1})	α_σ (d^{-1})	SSRs	R^2	ξ(m)	θ_{im} (v v^{-1})	λ (day^{-1})	α_σ (d^{-1})	SSRs	R^2
A	0.016	0.245	0.026	0.437	0.581	0.006	0.181	0.753	0.026	0.470	0.530
C	0.547	0.335	0.037	0.501	0.559	0.254	0.330	0.359	0.013	0.518	0.498
D	0.179	0.316	0.014	0.537	0.468	0.005	0.353	0.300	0.001	0.508	0.493
F	0.031	0.254	0.403	0.324	0.892	0.042	0.100	0.715	0.027	0.567	0.436

The changes in soil hydraulic properties appear to have occurred over a period of time during the post-DSE application period. This is reflected in the fact that predicted soil water contents do not fit observations equally well for the post-DSE application data and are commonly under-predicted in the initial stage (Figs. 4 and 5). If the soil hydraulic properties were constant, the model should fit all data equally well as it does for the pre-DSE application data (Fig. 2).

While the single-porosity flow model failed to simulate water contents for the post-DSE application period for lysimeters B and E, application of the dual-porosity model to these data was successful. Unlike the other four lysimeters under spray irrigation, these two were under flood irrigation, thus preferential flow is expected to be more significant. A dye tracer experiment and destructive sampling at the end of the field experiments (Jiang et al., 2008) revealed that there were more macropores in these two lysimeters than in other lysimeters. The dual-porosity model also yielded decreased values of θ_s and increased values of K_s for the post-DSE application period (Table 3) than those predicted from the pre-DSE application period (Table 2). This is in consistent with the findings for other lysimeters, as discussed earlier. For K_s it is appropriate to compare results from both flow models as K_s applies to the macropore domain only. However, it is difficult to compare other parameters derived from two different models. Unfortunately, the dual-porosity model failed to simulate water contents obtained from pre-DSE application for lysimeters B and E. Thus apart from K_s, we are unable to directly compare model results for assessing the changes in soil hydraulic properties of lysimeters B and E during the post-DSE application period. Nevertheless the success vs. failure in using different flow models for the pre- and post-DSE application periods suggests a significant change in soil hydraulic properties.

3.2. *Br and fecal coliform transport*

MIM-predicted Br and bacterial concentrations match well with most of those observed (Figs. 6–9). However the predicted peak bacterial concentrations for all lysimeters are significantly lower than those observed. This is because an equal weight was assigned in the model for all observed data during optimization. As there were many more data with low concentrations, modeling results are very much affected by the data with lower concentrations.

Bacterial breakthrough was either earlier than or at the same time as Br concentrations. The time for the peak Br and bacterial concentrations is 20 min (same time as DSE application) for lysimeter C and 6 days (same time as 1st irrigation) for lysimeters A and D. For lysimeters B, E and F, the time for the peak bacterial concentration is 6–7 days while for Br it is 18–20 days, about three times slower. This suggests that bacteria were not retarded in the soils and our assumption of negligible instantaneous sorption made in MIM is reasonable. Instead, bacterial transport could be faster than Br as a result of pore-size exclusion.

We believe that the rapid leaching of Br and bacteria in lysimeter C immediately (20 min) after DSE application and before any water irrigation is through a preferential flow path that penetrated most or all of the lysimeter depth. At that time, bacterial concentration in the leachate was 85% of the DSE applied (see C/C_o in Fig. 7). This indicates that applied DSE leached through preferential flow paths with little or no dilution. The topsoil of this lysimeter had a higher clay content, which readily forms preferential flow paths by shrinking and cracking. The greater risk of microbial leaching through structured clayey soils is also highlighted in Pang et al. (2008) and Pang (2009) who analyzed studies carried out both in New Zealand and overseas on microbial transport through intact soils.

For all lysimeters, bacterial leaching occurred at the start of the first irrigation event and their concentrations dropped rapidly as irrigation continued. In contrast, Br leaching had a relatively slower response to irrigation events. The MIM simulated well these different leaching patterns. The explanation for these distinct patterns is that the initial part of the flow event is dominated by drainage from large pores (Hallberg et al. 1986), which were followed by both Br and

Table 5 – Transport parameters optimized from observed Br and bacterial concentrations using the mobile-immobile transport model and dual-porosity flow model for lysimeters B and E.

Lysimeter	Br				Fecal coliform				
	ξ(m)	α_σ	SSRs	R^2	ξ(m)	λ (day^{-1})	α_σ	SSRs	R^2
B	0.049	0.051	0.403	0.561	0.151	0.589	0.040	0.288	0.713
E	0.017	0.077	0.421	0.680	4.88E-04	0.706	0.729	0.908	0.187

bacteria. As drainage slows down, much of the water being delivered to the lysimeter base is from smaller pores, and dominated by Br as the bacteria would be excluded or removed by the small pores. Compared to other lysimeters, Br leaching from lysimeters B and E responded well to irrigation events as more macropores were developed, and MIM simulated well these individual responses (Fig. 8).

Unlike in other lysimeters in which bacteria concentrations declined over time, there were abnormal rises of bacterial concentration in lysimeter E with irrigation events (Fig. 9). The reason is unclear but the possible explanations are (a) an external fecal source (e.g. from bird faeces), (b) release of entrapped bacteria due to soil structure change, and (c) under suitable nutrient state, bacteria growth during summer. The MIM is unable to simulate these abnormal increases of bacterial concentrations. As a result, the goodness of fit parameters (*SSR*s and R^2) for modeling of bacterial transport in lysimeter E is poor (Table 5). In trying to simulate these abnormal rises in bacterial concentrations, MIM produced a very high and probably unrealistic value of mass exchange coefficient (α_s).

Similar to the situation for water contents mentioned in Section 3.1.2, there are some under-predictions of Br and bacterial concentrations (Figs. 6–9) for the initial-stage simulations. Again we believe this discrepancy is a result of changes in soil structure, while the MIM assumes constant mobile and immobile regions for the whole simulated process (Mitchell and van Genuchten, 1991).

Compared to Br, values of dipersivity (ξ), immobile water content (θ_{im}), and mass exchange coefficient (α_s) determined from bacterial data are generally smaller (Table 4), indicating a significantly narrow pore-network and less mass exchange between mobile and immobile water zones in bacterial transport. This suggests that bacteria took short-circuit paths by preferential flow, consistent with pore-size exclusion theory (Ginn, 2002; Sinton et al., 2005).

4. Conclusions and recommendations

Our modeling results suggest that the single-porosity flow model is sufficient and adequate for simulating water movement through structured sandy loam soils under natural climatic conditions and spray irrigation (50 mm fortnightly in this study). However, a dual-porosity flow model is more appropriate for simulating water movement under flood irrigation (100 mm fortnightly in this study) as the effect of preferential flow paths becomes more significant under flood irrigation.

This study has demonstrated that soil structure and thus soil hydraulic properties can change with irrigation (especially under high hydraulic loading like flood irrigation), and with climate conditions. Thus parameter values that best describe water flow and contaminant transport under one set of conditions may not be applicable for another set of conditions. This dynamic change of soil structure needs to be considered.

Compared to soils with less topsoil clay and soils under spray irrigation, soils with higher topsoil clay content and soils under flood irrigation have a greater risk of bacterial leaching through preferential flow paths, potentially impairing groundwater quality. Management strategies to reduce bacterial leaching from land application of effluent must aim to minimize the effect of preferential flow by adopting appropriate irrigation schemes, e.g. using spray instead of flood irrigation and decreasing DSE application depth but increasing irrigation frequency. Special attention is needed to use of a low irrigation rate at the beginning of each irrigation event (particularly if the soils are very dry) to allow sufficient time for soil to wet up and swell for more effective water retention so that bacterial leaching can be minimized.

Acknowledgements

We thank the New Zealand Foundation for Research, Science and Technology and the Institute of Environmental Science & Research for funding this research with Scholarships, and the Centre for Soil and Environmental Quality for providing lysimeters and technical support.

REFERENCES

Aislabie, J., Smith, J., Fraser, R., McLeod, M., 2001. Leaching of bacterial indicators of faecal contamination through four New Zealand soils. Australian Journal of Soil Research 39 (6), 1397–1406.

American Public Health Association, American Water Works Association and Water Environment Federation, 1998. Standard Methods for the Examination of Water and Waste Water. American Public Health Association, Washington, DC.

Bradford, S.A., Šimůnek, J., Walker, S.L., 2006. Transport and straining of *E. coli* O157:H7 in saturated porous media. Water Resources Research 42, W12S12,. doi:10.1029/2005WR004805.

Brown, C.D., Hollis, J.M., Bettinson, R.J., Walker, A., 2000. Leaching of pesticides and a bromide tracer through lysimeters from five contrasting soils. Pest Management Science 56, 83–93.

Chen, C., Roseberg, R.J., Selker, J.S., 2002. Using microsprinkler irrigation to reduce leaching in a shrink/swell clay soil. Agricultural Water Management 54, 159–171.

Close, M., Dann, R., Ball, A., Pirie, R., Savill, M., Smith, Z., 2008. Microbial groundwater quality and its health implications for a border-strip irrigated dairy farm catchment, South Island, New Zealand. Journal of Water and Health 6 (1), 83–98.

Edwards, W.M., Shipitalo, M.J., Owens, L.B., Dick, W.A., 1993. Factors affecting preferential flow of water and atrazine through earth-worm burrows under continuous no-till corn. Journal of Environmental Quality 22, 453–457.

Feddes, R.A., Kowalik, P.J., Zaradny, H., 1978. Simulation of Field Water Use and Crop Yield. Wageningen, The Netherlands.

Flury, M., Yates, M.V., Jury, W.A., 1999. Numerical analysis of the effect of the lower boundary condition on solute transport in lysimeters. Soil Science Society of America Journal 63, 1493–1499.

Gargiulo, G., Bradford, S.A., Simunek, J., Ustohal, P., Vereecken, H., Klumpp, E., 2008. Bacteria transport and deposition on under unsaturated flow conditions: the role of water content and bacteria surface hydrophobicity. Vadose Zone Journal 7, 406–419.

Gerke, H.H., van Genuchten, M.T., 1993. A dual-porosity model for simulating the preferential movement of water and solutes in structured porous media. Water Resources Research 29 (2), 305–320.

Gerke, H.H., van Genuchten, M.T., 1996. Macroscopic representation of structural geometry for simulating water

and solute movement in dual-porosity media. Advances in Water Resources 19 (6), 343–351.
Ginn, T.R., 2002. A travel time approach to exclusion on transport in porous media. Water Resources Research 38 (4), 12.01–12.12.
Guber, A.K., Shelton, D.R., Pachepsky, Y.A., 2005. Transport and retention of manure-borne coliforms in soil. Vadose Zone Journal 4 (3), 828–837.
Hallberg, G.G., Baker, J.L., Randall, G.W., 1986. Utility of Tile-line Effluent Studies to Evaluate the Impact of Agricultural Practice on Ground Water. National Water Well Assoc., Dublin, OH/ Omaha, NE, pp. 298–326.
Hay, R.K.M., Porter, J.R., 2006. The Physiology of Crop Yield Ames. Iowa: Blackwell Pub., Oxford, UK.
Hekman, W.E., Heijnen, C.E., Burgers, S.L.G.E., van Veen, J.A., van Elsas, J.D., 1995. Transport of bacterial inoculants through intact cores of two different soils as affected by water percolation and the. FEMS Microbiology Ecology 16 (2), 143–157.
Hijnen, W., Brouwer-Hanzens, A., Charles, K., Medema, G., 2005. Transport of MS2 phage, *E. coli, Clostridium perfringens, Cryptosporidium parvum* and *Giardia intestinalis* in a gravel and a sandy soil. Environmental Science and Technology 39, 7860–7868.
Jarvis, N.J., 2007. A review of non-equilibrium water flow and solute transport in soil macropores: principles, controlling factors and consequences for water quality. European Journal of Soil Science 58, 523–546.
Jiang, S., Buchan, G.D., Noonan, M.J., Smith, N., Pang, L., Close, M., 2008. Bacterial leaching from dairy shed effluent applied to a fine sandy loam under irrigated pasture. Australian Journal of Soil Research 46, 552–564.
Lin, H., Zhou, X., 2008. Evidence of subsurface preferential flow using soil hydrologic monitoring in the Shale Hills catchment. European Journal of Soil Science 59, 34–49.
Ludlow, M.M., 1985. Photosynthesis and dry matter production in C3 and C4 pasture plants, with special emphasis on tropical C3 legumes and C4 grasses. Australian Journal of Plant Physiology 12, 557–572.
McGechan, M.B., Vinten, A.J.A., 2003. Simulation of transport through soil of *E. coli* derived from livestock slurry using the MACRO model. Soil Use and Management 19 (4), 321–330.
McLaren, R.G., Cameron, K.C., 1996. Soil Science: Sustainable Production and Environmental Protection. Oxford University Press, Auckland, NZ.
McLeod, M., Aislabie, J., Smith, J., Fraser, R.H., Robert, A., Taylor, M.D., 2001. Viral and chemical tracer movement through contrasting soil. Journal of Environmental Quality 30 (6), 2134–2140.
McLeod, M., Aislabie, J., Ryburn, J., McGill, A., Taylor, M.D., 2003. Microbial and chemical tracer movement through two Southland soils, New Zealand. Australian Journal of Soil Research 41 (6), 1163–1169.
McLeod, M., Aislabie, J., Ryburn, J., McGill, A., 2004. Microbial and chemical tracer movement through Granular, Ultic and Recent Soils. New Zealand Journal of Agricultural Research 47 (4), 557–563.
McMurry, S.W., Coyne, M.S., Perfect, E., 1998. Fecal coliform transport through intact soil blocks amended with poultry manure. Journal of Environmental Quality 27 (1), 86.
Mitchell, A.R. and van Genuchten, M.T., 1991. Preferential Flow. Gish, T.J. and Shirmohammadi, A. (eds), pp. 278–287, Am. Soc. Agric. Eng., St. Joseph, MI.
Mualem, Y., 1976. A new model for prediction of the hydraulic conductivity of unsaturated porous media. Water Resources Research 12 (3), 513–522.
Pang, L., Mcleod, M., Aislabie, J., Simunek, J., Close, M., Hector, R., 2008. Modeling transport of microbes in ten undisturbed soils under effluent irrigation. Vadose Zone Journal 7 (1), 97–111.
Pang, L., 2009. Microbial removal rates in subsurface media estimated from published studies of field experiments and large intact soil cores. Journal of Environmental Quality 38, 1531–1559.
Ritchie, J.T., 1972. Model for predicting evaporation from a row crop with incomplete cover. Water Resources Research 8 (5), 1204–1213.
Schaap, M.G., Leij, F.J., van Genuchten, M.T., 2001. Rosetta: a computer program for estimating soil hydraulic parameters with hierarchical pedotransfer functions. Journal of Hydrology 251, 163–176.
Shelton, D.R., Pachepsky, Y.A., Sadeghi, A.M., Stout, W.L., Karns, J.S., Gburek, W.J., 2003. Release rates of manure-borne coliform bacteria from data on leaching through stony soil. Vadose Zone Journal 2 (1), 34–39.
Šimůnek, J., Jarvis, N.J., van Genuchten, M.T., Gärdenäs, A., 2003. Review and comparison of models for describing non-equilibrium and preferential flow and transport in the vadose zone. Journal of Hydrology 272, 14–35.
Šimůnek, J., Sejna, M., Van Genuchten, M.T., 1998. The HYDRUS-1D Software Package for Simulating the One-Dimensional Movement of Water, Heat, and Multiple Solutes in Variably-saturated Media: Version 2.0. IGWMC-TPS-70. International Ground Water Modeling Center. Colorado School of Mines, Golden.
Šimůnek, J., van Genuchten, M.T., 2006. The Handbook of Groundwater Engineering. In: Delleur, J.W. (Ed.). CRC Press Boca Raton, FL, pp. 22.21–22.46.
Šimůnek, J., van Genuchten, M.T., 2008. Modeling nonequilibrium flow and transport processes using HYDRUS. Vadose Zone Journal 7 (2), 782–797.
Šimůnek, J., Van Genuchten, M.T., Sejna, M., 2005. The HYDRUS-1D Software Package for Simulating the One-dimensional Movement of Water, Heat and Multiple Solutes in Variably-saturated Media. Department of Environmental Sciences, University of California Riverside, Riverside, California.
Šimůnek, J., Wendroth, O., Wypler, N., van Genuchten, M.T., 2001. Non-equilibrium water flow characterized by means of upward infiltration experiments. European Journal of Soil Science 52, 13–24.
Sinton, L.W., Braithwaite, R.R., Hall, C.H., Pang, L., Close, M.E., Noonan, M.J., 2005. Tracing the movement of irrigated effluent into an alluvial gravel aquifer. Water Air and Soil Pollution 166, 287–301.
Smith, M.S., Thomas, G.W., White, R.E., Ritonga, D., 1985. Transport of *Escherichia coli* through intact and disturbed soil columns. Journal of Environmental Quality 14 (1), 87–91.
Torkzaban, S., Tazehkand, S.S., Walker, S.L., Bradford, S.A., 2008. Transport and fate of bacteria in porous media: Coupled effects of chemical conditions and pore space geometry. Water Resources Research 44. doi:10.1029/ 2007WR006541.
van Genuchten, M.T., 1980. A closed-form equation for predicting the hydraulic conductivity of unsaturated soils. Soil Science Society of America Journal 44, 892–898.
van Genuchten, M.T., Leij, F.J., Yates, S.R., 1991. Version 1.0. The RETC Code for Quantifying the Hydraulic Functions of Unsaturated Soils. U.S. Salinity Laboratory USDA, ARS, Riverside, CA.
van Genuchten, M.T., Šimůnek, J., 2004. Unsaturated-Zone modeling; Progress, Challenges and applications, Wageningen UR frontis series. In: Feddes, R.A., de Rooij, G.H., van Dam, J.C. (Eds.). Kluwer Academic Publishers, Dordrecht, The Netherlands, pp. 37–69. x–xi.
van Genuchten, M.T., Wagenet, R.J., 1989. Two-site/two-region models for pesticide transport and degradation: theoretical development and analytical solutions. Soil Science Society of America Journal 53 (5), 1303–1310.